Nano Energy 77 (2020) 105201

Contents lists available at ScienceDirect

Nano Energy

journal homepage: http://www.elsevier.com/locate/nanoen

An effective self-powered strategy to endow titanium implant surface with associated activity of anti-biofilm and osteogenesis

Rui Shi [a], Jingshuang Zhang [a], Jingjing Tian [b,f], Chaochao Zhao [b], Zhe Li [b], Yingzi Zhang [c], Yusheng Li [d], Chengai Wu [a], Wei Tian [a,e,**], Zhou Li [b,*]

[a] Beijing Laboratory of Biomedical Material, Beijing Institute of Traumatology and Orthopaedics, Beijing Jishuitan Hospital, Beijing, 100035, China
[b] CAS Center for Excellence in Nanoscience, Beijing Key Laboratory of Micro-nano Energy and Sensor, Beijing Institute of Nanoenergy and Nanosystems, Chinese Academy of Sciences, Beijing, 100083, China
[c] Department of Orthopedics, The Second Affiliated Hospital of Soochow University, Suzhou, Jiangsu, 215000, China
[d] Department of Orthopaedics, Xiangya Hospital, Central South University, Changsha, Hunan Province, 410008, China
[e] Department of Spine Surgery, Peking University Fourth School of Clinical Medicine, Beijing, 100035, China
[f] Central Laboratory, Peking Union Medical College Hospital, Peking Union Medical College and Chinese Academy of Medical Sciences, Beijing, 100730, China

ARTICLE INFO

Keywords:
Implant
Anti-biofilm
Osteogenesis
Self-powered
Triboelectric nanogenerator

ABSTRACT

The implant-associated infections will cause implant failure, which bring patient suffering and risk of infection death. Once forming bacteria biofilms on implant, the resistance to antibiotics will increase hundreds of times. However, the recent methods that endow implant with antibacterial activity, are always time-limited, process complicated, unstable, introducing new antibacterial components with side effects and showing little effect on mature bacterial biofilm. Meanwhile, some method may inhibit osteoblasts' adhesion and suppress osteogenesis. Here, we present a self-powered method of loading and accumulating negative charges on the surface of anodized titanium implant by using a triboelectric nanogenerator (TENG). The most obvious advantage is that TENG can harvest and transfer mechanical energy from daily human motions to electrical energy for building the stable and long-term effective negatively charged implant surface, which effectively inhibits bacterial adhesion, reduces bacteria number and lowers the live/dead bacteria ratio in forming and mature biofilms. Moreover, the treated implant reveals osteogenesis promotion in MC3T3-E1 cells, without adverse side effects. Our findings provide a promising method for energizing implant with *anti*-biofilm and osteogenesis promotion activity by self-powered technology in vivo, which may also encourage new design impetus for multi-functional material as implant and for medical devices in future.

1. Introduction

Titanium and its alloys are the widely used materials applied for manufacturing orthopedic or dental implants owing to their good mechanical strength, biocompatibility, and corrosion resistance [1]. Typical titanium based long-term implants are expected to serve over ten years [2]. Over such a long service lifetime, implant-associated infections are one of the main causes of implant failure.

Currently, the risk of global infection in orthopedic surgery is 2%–5% [3]. These implant-associated infections caused as planktonic bacteria first adhere to the device surface and ultimately developed into biofilms [4]. Bacteria in biofilms are resistant to antibiotics at levels 500–5000 times higher than those needed to kill floating bacteria [5], so the infections are difficult to eliminate. The biofilm caused infections always lead to poor osseointegration and implant failure. There are numerous solutions for imparting titanium surfaces with antibacterial properties. Common strategies such as surface modification and coating using antibacterial macromolecules [6–8], antimicrobial peptides [9], antibacterial metal elements [10], and antibiotics [11,12] have been produced to introduce antibacterial properties [3]. Some of these strategies interfere with the initial bacterial adhesion stage of biofilm formation, while others exhibit direct bacterial killing properties [13].

* Corresponding author.
** Corresponding author. Beijing Laboratory of Biomedical Material, Beijing Institute of Traumatology and Orthopaedics, Beijing Jishuitan Hospital, Beijing, 100035, China.
E-mail addresses: tianweijst@vip.163.com (W. Tian), zli@binn.cas.cn (Z. Li).

https://doi.org/10.1016/j.nanoen.2020.105201
Received 18 June 2020; Received in revised form 9 July 2020; Accepted 15 July 2020
Available online 19 July 2020

However, to date, no treatment can effectively destroy biofilm or prevent it recurrence.

Recently, surface charge has been applied as a new antibacterial functionalization strategy. It has been reported that both positive and negative surface charge have the ability to inhibit the adherence of gram-negative bacteria to the surfaces of different materials and promote antibacterial efficiency [14–18]. Some studies reveal that the antibacterial mechanism should be the surface charges can disturb the membrane potential, which leads to irreversible damages in the membrane structure [19,20]. In general, cytomembrane of microorganism contains a large number of carboxyl and phosphate groups that endow their membrane a negative surface charge at neutral pH [21]. Therefore, negatively charged bacteria are less likely to adhere to the negative implant surface owing to electrostatic repulsion. It was reported that positively charged surfaces are difficult to inhibit the formation of bacterial biofilms in a long time, while negatively charged surfaces deter biofilm formation more effectively even after 70 h [21]. However, a major drawback of the existing methods for creating negatively charged surfaces is that it is challenging to meet the demand of long-acting bacteriostasis throughout the full life cycle of the implant. There is therefore an urgent need for new ways of creating negative implant surfaces that can play a long-term bacteriostatic role.

In addition to implant-associated infections, lack of initial bone-binding capacity due to the biological inert of the materials always results in implant failures [22,23]. To address this problem, researchers have tried different methods for modifying the Ti-based implants surfaces' structure and chemistry while maintaining their excellent bulk properties, such as preparing bio-mimic implant surface [24,25] and tailoring the roughness of surface [26–28]. Creating titanium dioxide (TiO_2) nanotubes on the Ti surface has been demonstrated to induce significantly greater osteogenesis compared with unmodified Ti plates [29]. Recently, some studies proved that stimulation by direct current [30], pulse electric current [31], electric and electromagnetic fields [17,18] can all promote osteoblast proliferation and differentiation [32,33]. Thus, we infer that the osteogenesis of Ti implant surfaces can be improved by first constructing TiO_2 nanotubes on the surface and then introducing electrical stimulation. However, identifying an external power source that satisfies the miniaturization and weight reduction requirements for osseointegration of implantable medical devices is also a major issue.

Advances in bioelectronics have enabled progress in the use of body-electric closed-loop system for treating long-term diseases [34]. In order to solve the problem of long-term power supply for implantable devices, some research groups have focused on the self-sustainable power source to remove the batteries from the system, negating the periodical maintenance service [35,36]. TENGs as self-powered electronics are getting more and more attention in the collection and conversion of energy produced by organisms [37–39]. The TENGs provide us an effective way to transform mechanical energy available in our daily life but fail to take advantage of—such as breathe, walking, vibration, eye motion, hart beating—into electric energy [40–42]. Thus, TENGs can act as implantable and sustainable power sources to charge medical devices. It has been reported that the TENG has been used to collect breathing and heart beat energy of a mouse to charge a pacemaker [43–45]. It also acts as a pulse sensor with high sensitivity [46,47] and a wireless transmission device [48,49]. Although the TENG was utilized to charge titanium dioxide nanotubes doped with carbon to kill bacteria, this study was focused on the post-charging antibacterial effects proportional to the capacitance [18]. There is no report of using of TENG to inhibit orthopedic implant-related infections while simultaneously promoting bone formation on the surface of the implants.

In this study, the energy generated by human daily exercise was converted into electricity by a TENG, which produced a negative voltage after rectification to act on the anodized titanium implants. The formation and development of bacterial biofilms, the destruction of mature bacterial biofilms, and the promotion of surface osteogenesis were systematically studied to establish the effect of the TENG negatively charged surface. The results of this study demonstrate a new solution for simultaneously endowing the surface of implant with antimicrobial properties and promoting bonding between the bone tissue and the implant, which is crucial for sustainable *anti*-biofilm activity and osteogenesis of orthopedic and dental implants. This work also encourages new design impetus for multi-functional material as implant and for medical devices in future.

2. Experimental section

2.1. Samples and electrical stimulation device

2.1.1. Preparation of Ti-based samples

All of the pure titanium (Ti) plates were commercially available (cpTi, grade 2, Titanium Industries, Inc.) and were cut into several plates with a size of 4 cm × 8 cm. The TiO_2 nanotubes (TNT) were prepared by electrochemical anodization of a Ti plate in an NH_4F-ethylene glycol solution, containing H_2O (10%), NH_4F (0.5%), and ethylene glycol (89.5%, Beijing Chemical Works, China). The Ti plates were ground with abrasive paper (from 400 to 2000 grit), cleaned ultrasonically in acetone, alcohol (Beijing Chemical Works, China), and deionized water, and dried in nitrogen. Anodization was performed at 50 V for 3 h at room temperature (25 °C) in a conventional two-electrode cell with a DC power supply (IT6123, ITECH, Nanjing, China). The pure and anodized Ti plates with TiO_2 nanotubes were cut into discs with a diameter of 11 mm using a laser. Finally, the anodized discs were annealed in argon at 450 °C for 3 h. The side and back of both the unmodified Ti and TNT discs were encased in PDMS to avoid charge loss from the back and side of the discs. TNT discs were both used for the fabrication of TENG and negative electrode of electrical stimulation device for experimental cell and bacteria surface.

2.1.2. Fabrication of the TENG

Fabrication of the TENG was based on vertical contact separation. The inner face of a polytetrafluoroethylene (PTFE) film was etched with nanorods and the anodized inner face of the Ti foil with nanotubes was used as triboelectric layers (Fig. 1a). Copper with a thickness of 200 nm was magnetron sputtered onto the exterior face of the PTFE film to give one electrode and the exterior face of the Ti foil without anodization was used as the other electrode. The naked TENG was encapsulated in PTFE tape and subsequently in polydimethylsiloxane (PDMS). A periodical compressive force with a frequency of 1.25 Hz was applied to the TENG. The open-circuit voltage, short-circuit current, and transferred charge of the TENG were measured using an electrometer (Keithley 6517B, USA) and a digital oscilloscope (Keithley DPO6450, USA).

2.1.3. Electrical stimulation device

Before culturing with bacteria or cells, the anodized titanium discs were washed with ethanol and sterilized by autoclaving. To fix the Ti and TNT discs to the 24-well plates, 3D printed supports were used, which were connected to the anode and cathode of the TENG after rectification by thin copper wires (Fig. 2d). The charge and discharge properties of the device were characterized using an electrochemical workstation (CHI660, China). The discs were kept vertical to the bottom of the 24-hole plate to eliminate the effects of gravity on the bacteria, as shown in Supplementary Fig. 1. The distance between the pure Ti and TNT discs in each well was ~5 mm. In the cell experiment, the TNT discs were placed parallel to the bottom of the 24-well plates. To ensure that the distance between the Ti plate and the TNT plate was equal in each hole, we used a 3D printed rod as a support between the two plates. The device in the cell plate before stimulation is shown in Supplementary Fig. 2.

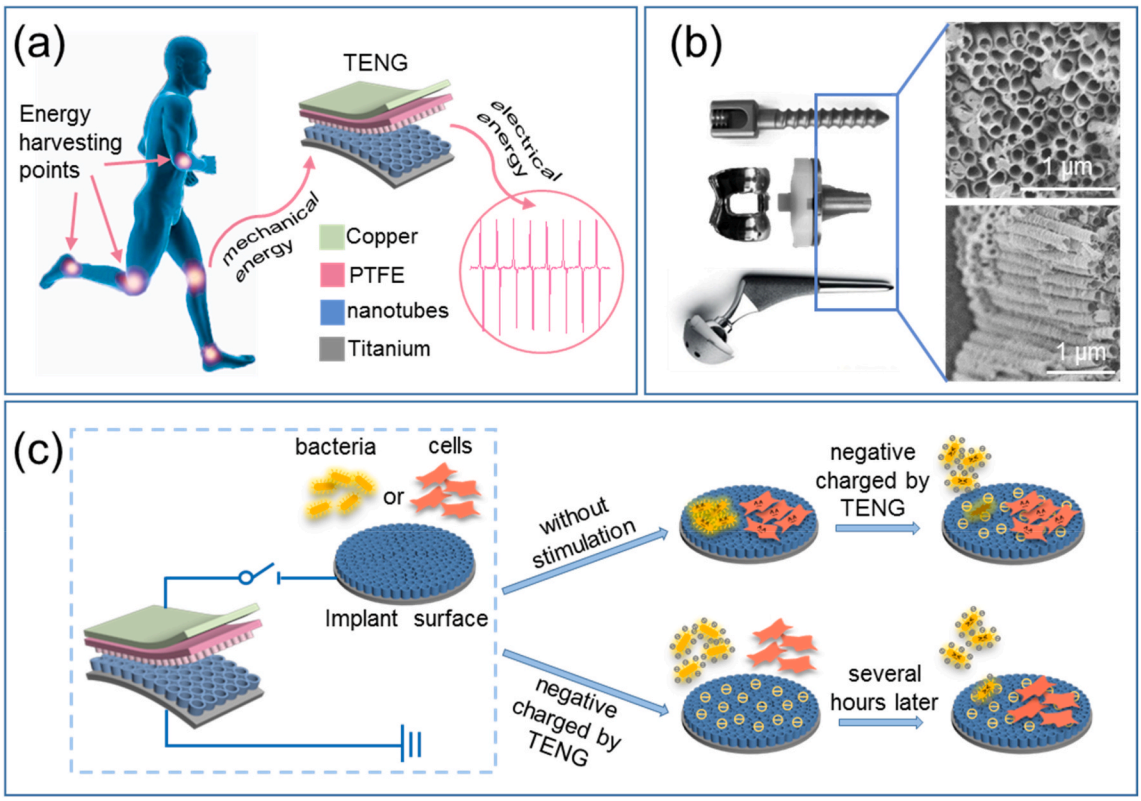

Fig. 1. Mode of action and mechanism of TENG in the construction of antimicrobial and osteogenesis promoting surfaces for orthopedic or dental implants. (a) Energy harvesting points of the human body and the structure of TENG. (b) Surface morphology of Ti orthopedic implants after anodic oxidation. (c) Assumed principle of biofilm formation inhibition and promotion of osteogenic differentiation.

2.2. Evaluation of antibacterial performance

The ability to prevent biofilm formation was assessed with two model bacteria, *Escherichia coli* (*E. coli*) (CICC 23657) and *Staphylococcus aureus* (*S. aureus*) (CICC 10384). The bacteria were cultured in nutrient broth at 37 °C for 12 h to the logarithmic phase in a 120 rpm shaker. The bacteria solution was then centrifuged at 8000 rpm and resuspended in sterilizing nutrient broth to reach a concentration of 1×10^3 or 1×10^6 CFU mL^{-1} before being inoculated in 24-well culture plates. The samples were divided into two groups: without stimulation (control) and with TENG stimulation (TENG).

2.2.1. Effect of TENG stimulation on the initial bacterial adhesion and maturity

After different periods of stimulation (1, 2, 3, and 4 h) with an initial concentration of 1×10^3 CFU mL^{-1}, the bacteria on the surface of the TNT disc and in solution were quantified using the colony counting method. After stimulating for 2, 4, 8, 24, 48, and 72 h with an inoculation concentration of 1×10^6 CFU mL^{-1}, the biofilm formed on the TNT was semi-quantified using crystal violet staining. In addition, the morphology and distribution of the biofilms formed on the TNT were observed by scanning electron microscopy (SEM) and confocal laser scanning microscopy (CLSM).

2.2.2. Effect of TENG stimulation on the elimination of formed biofilms

The bacteria were inoculated in 24-well plates at a concentration of 1×10^6 CFU mL^{-1} and cultured for 24 h. There was one TNT disc in each well. The TNT samples were then taken out and rinsed gently before being put into new wells with sterilized nutrient broth. After treating with antibiotics (AB, penicillin for *S. aureus* and streptomycin for *E. coli*), TENG stimulation, or AB combined with TENG for 24 h, the samples were assessed using crystal violet staining or LIVE/DEAD staining. The bacteria in the solution were quantified using the colony counting method.

2.2.3. Colony counting method

The bacterial solution was centrifuged at 8000 rpm, resuspended in PBS, and then uniformly inoculated in solid medium plates after gradient dilution. Two plates were used at each concentration, and colony counting was conducted after 24 h of culture in a constant temperature incubator at 37 °C. To measure the bacteria on the TNT discs, each TNT disc was pressed five times onto a dish, then the dish was incubated for 24 h to count the colonies.

2.2.4. Crystal violet staining

The TNT discs were rinsed with PBS three times to remove planktonic bacteria, and fixed with anhydrous methanol (Beijing Chemical Works, China) for 10 min. The methanol was removed with a pipette and then the discs were stained with crystal violet solution (0.1%, Solarbio, China) for 15 min. The discs were then gently washed with running water and immersed in ethanol (95%) for 15 min to dissolve the stained biofilms. The optical density value was measured at 570 nm.

2.2.5. Morphology observation using SEM

At predetermined time points, half of the TNT samples were taken out, rinsed three times with PBS, fixed with glutaraldehyde (2.5%) at 4 °C overnight, and dehydrated in a series of ethanol solutions (50%, 70%, 80%, 90%, and 100%) for 15 min successively, and in anhydrous ethanol a further twice. The samples were then dried, platinum coated, and scanned using SEM.

2.2.6. LIVE/DEAD staining

The other half of the samples were also rinsed with PBS three times, and stained with LIVE/DEAD dye solution for 15 min before being

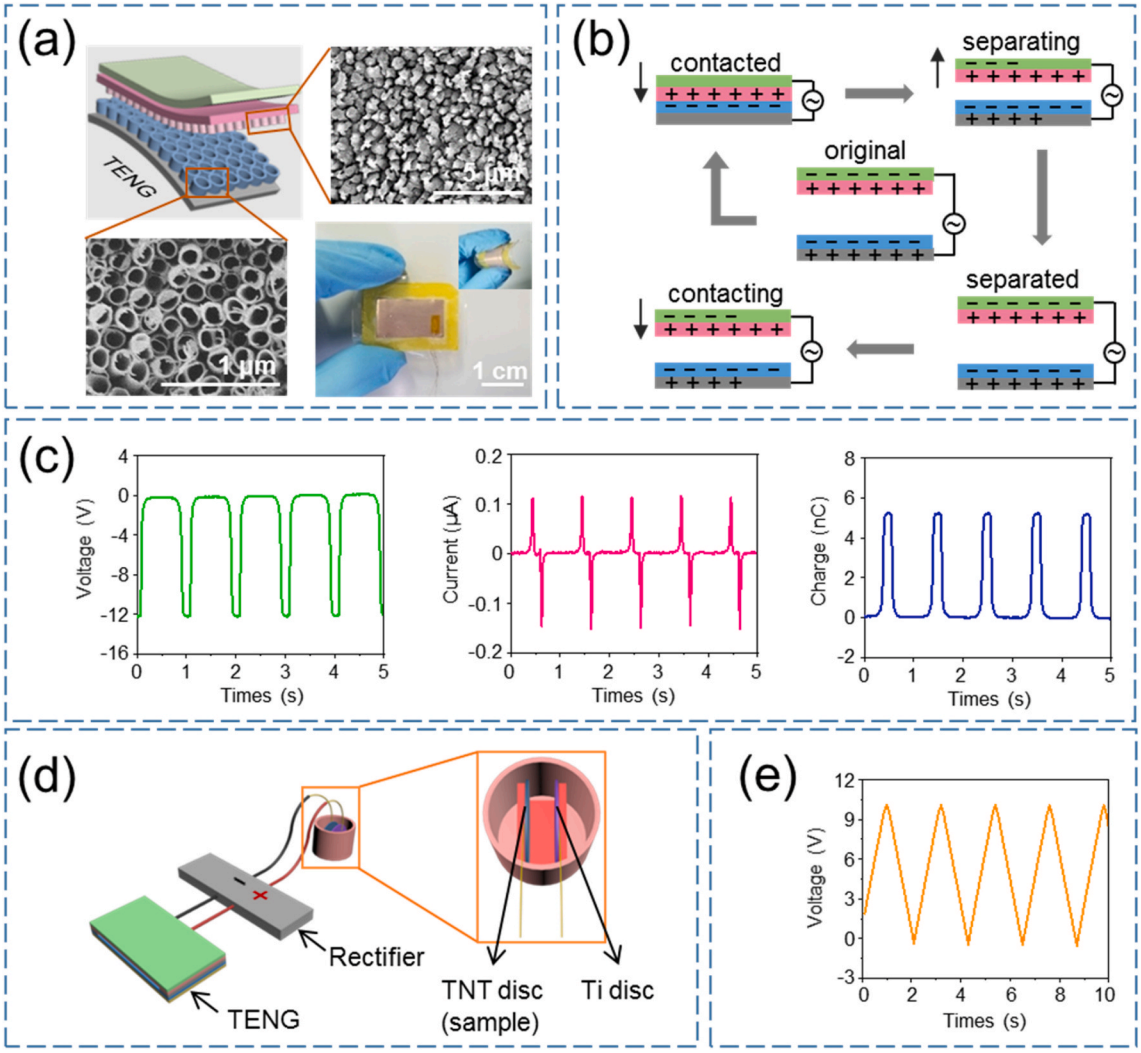

Fig. 2. Working principle and output signals of TENG and the whole experimental device. (a) Surface microstructure of the friction layers and general appearance of TENG. (b) The working mode of contact-separated TENG. (c) The open-circuit voltage, short-circuit current, and charge quantity of TENG. (d) Schematic diagram of experimental devices, and (e) capacitive character of the pair of the discs in each well.

observed with CLSM. The dye solution contained the same amount of SYTO 9 and PI. Live bacteria stained with SYTO9 show green fluorescence, while dead bacteria stained with PI show red fluorescence. The amounts of live and dead bacteria were expressed by average fluorescence density, which was analyzed by ImageJ software.

2.3. Evaluation of cell performance

MC3T3-E1 cells were obtained from the American Type Culture Collection (ATCC). The cells were cultured and expanded in α-MEM medium (Hyclone, USA) supplemented with 10% fetal bovine serum (FBS, Gibco) and 1% penicillin-streptomycin solution (100 × , Solarbio, China).

2.3.1. Cytotoxicity and proliferation

MC3T3-E1 cells in the logarithmic growth phase were harvested, centrifuged, and resuspended in sterilized fresh α-MEM medium at a density of 1×10^4 cells mL^{-1}. After adherence to the Ti or TNT discs in the 24-well culture plates, the samples were divided into four groups, including samples without stimulation (Ti and TNT), negatively charged TNT samples stimulated by TENG (TENG−), and positively charged TNT samples stimulated by TENG (TENG+). Ti discs were used as the basic blank control. The cell viability and proliferation were measured by CCK-8 assay. After treatment for 1, 3, 5, and 7 d, the medium was replaced with fresh medium containing CCK-8 solution (10%) and the samples were incubated for 3 h. The optical density was determined on a multimode reader (Bio Tek, USA) at 450 nm. At the 5 d stimulation time point, half of the Ti/TNT discs with cells on the surface were fixed with paraformaldehyde (PFA, 4%) for 10 min, permeabilized with Triton X-100 for (0.5%) 10 min, blocked with BSA (1%) for 30 min at 37 °C, stained with phalloidin-fluorescein isothiocyanate (FITC) (Sigma, USA) for 40 min at room temperature, and then stained with propidium iodide (PI) (Sigma, USA) for 15 min. PBS was used to remove excess reagents. Finally, the Ti/TNT samples were observed by CLSM. Other Ti/TNT discs were fixed with glutaraldehyde (2.5%) at 4 °C overnight, dehydrated in a series of ethanol solutions (50%, 70%, 80%, 90%, and 100%) for 15 min successively, then the samples were dried, platinum coated, and scanned by SEM.

2.3.2. Osteogenesis

MC3T3-E1 cells in the logarithmic growth phase were incubated in 24-well plates with one TNT disc in each well at a density of 2×10^4 cells mL^{-1}. After 48 h, the medium was replaced by fresh α-MEM medium supplemented with 10% FBS, 1% penicillin-streptomycin solution (100 ×), dexamethasone (0.1 mM, Sigma, USA), β-glycerophosphate (2.5 M, Sigma, USA) and L-ascorbic acid (50 mM, Amresco, USA). The cells were

treated in the following groups, no stimulation (TNT), TENG+, and TENG−. After 7 d, the cells were harvested with RIPA lysis buffer (Solarbio, China), centrifuged at 12,000 r/min for 5 min at 4 °C. The amount of total protein in the supernatant was quantified using a BCA Protein Assay Kit (Thermo, USA), and the activity of alkaline phosphatase (ALP) was detected using an ALP assay kit. After 21 d, the samples were rinsed twice with PBS, fixed with formalin (10%) for 10 min, stained with alizarin red S (0.2%) for 5 min, and observed by inverted microscopy.

2.4. Statistical analysis

The data were evaluated by a one-way analysis of variance (ANOVA). The data are shown as mean ± SD ($n = 3$) and $P < 0.05$ was considered statistically significant. The statistical analysis was performed with IBM SPSS Statistics (Version 19.0, IBM Corp., Armonk, NY, USA).

3. Results and discussion

3.1. Performance of the experimental device

Implant-related infections often accompany the full life cycle of material implantation. The effective life cycle of many titanium alloy prostheses is 10–15 years. Avoiding bacterial colonization and preventing individual bacteria from developing into bacterial biofilms during such long service cycles is a clinical problem that has not yet been solved. It has been reported that most bacteria have negative surface charge at physiological pH [50], which introduces the possibility of electrostatic repulsive forces between the negatively charged bacteria and a negatively charged surface. Thus, bacterial adhesion on the surface of the material can be repelled. In addition, it has been shown that negatively charged surfaces not only inhibit the formation of bacterial biofilms [51], but also encourage bone marrow mesenchymal stem cell (BM-MSC) activity and osteogenic differentiation [52]. However, one of the main factors affecting the clinical application of electrical stimulation technology is the continuous generation of electric charge on the surface of titanium-based implants. General power sources have a limited service life; therefore, it is necessary to find new power supply equipment to charge the surface of the Ti-based implant.

There are several energy harvesting points in the human body for TENGs to capture kinetic energy and convert it into electricity as shown in Fig. 1a. The design of TENG should depend on the location of the implant. The TENG suitable for adhesion to joints can be prepared by referring to the methods in other studies [42,53]. By adhering or implanting TENG onto/into one or more sites that experiences constant movement, it can continuously release electrical charge to the implant surface. For titanium artificial joints, the hip joint handle can be used as the cathode of the device used in this study, and the metal plate in the external fixation device may acted as the other electrode. For other orthopedic implants, such as a titanium plate, the plate itself can be used as the cathode, and the metal plate in the opposite side or the external fixation device can be used as the anode. The detailed design should be established according to the shape and implant-position of the implants. However, Ti is a good conductor of electricity, therefore the charge injected into Ti implants can rapidly flow into the surrounding body fluid, which is also a good conductor. It is therefore difficult to accumulate charge on the surface of Ti-based implants to contribute to anti-infection activity. Anodizing the surface alters the elemental composition to TiO_2, which is not a conductor without specific stimulation. This prevents the charge injected into the titanium metal from transferring so rapidly to the body fluid, as it partially accumulates on the surface of the titanium dioxide nanotubes, endowing them with antibacterial function. Additionally, it has been shown that the formation of titanium nanotube arrays on Ti surfaces by anodic oxidation can promote osteoblast adhesion, proliferation, and differentiation [54], thus effectively promoting the integration of the implant surface and bone tissue. The surface of orthopedic titanium implants can be treated by anodic oxidation to create a TiO_2 nanotube layer on the surface of Ti. Fig. 1b shows the microstructure of the surface of an anodized titanium plate that was used in this study. The nanotubes were approximately 100 nm in diameter and approximately 2 μm in length.

In light of the above considerations, we put forward the hypothesis (Fig. 1c) that under the constant stimulation of a TENG, the negative charge would enrich the surface of anodized titanium to repel or kill adherent bacteria, which also have a negatively charged membrane. By using the mechanical energy generated by the human body—but not effectively used—combined with this new electrical power generation device, it is hoped that the formation of bacterial biofilms can be prevented, formed bacterial biofilms can be destroyed, the osteogenic ability of the implant surface can be promoted, and the loosening of the prosthesis can be prevented.

Fig. 2a exhibits the microstructure of the triboelectric layers of the TENG. The upper right image shows the nanorods on the PTFE plate, and the lower left image shows the TiO_2 nanotubes on the Ti plate. The size of the naked TENG we used was 1.6 cm × 1 cm, and became 2.6 cm × 2 cm after encapsulation, which is shown in the lower right picture of Fig. 2a. Fig. 2b illustrates the working principle of the TENG. The system operates by employing the coupling effects between triboelectrification that arise from contact and separation between the PTFE layer and TiO_2 layer. The power generation comes from the triboelectric effect that induces electrostatic charges on the surface of the triboelectric materials and results in electron flow between the electrodes. In the initial state, the system has no electric potential difference because there is no generated or induced charge. The introduction of external force to the system causes the triboelectric layers to come into contact, and charge transfer occurs as a result of triboelectrification. Fig. 2c shows the characteristics of the electrical signals generated using our TENG, including open-circuit voltage (12 V), short-circuit current (0.15 μA), and transferred charge (5.3 nC). The fatigue testing showed that the stable output voltage was maintained in 1 × 106 cycles (Supplementary Fig. 4.), which demonstrated the TENG used in this study has excellent stability and durability. The devices used in this electrical stimulation system and their interconnection are shown in Fig. 2d, and include a TENG, a rectifier, and some discs immersed in the medium culturing the bacteria or cells. Notably, the system in this research was designed to avoid the flow of exogenous current to the medium, which means the system behaves as a capacitive coupling device. The capacitive character of the target TNT discs was characterized by an electrochemical workstation as shown in Fig. 2e, which shows that it had good capacitance. It has previously been reported that the application of constant cathodic potentials to titanium significantly improves the antibacterial efficiency for the eradication of bacteria attached to the metal surface [51]. However, the specific focus of this study is whether the electrical signal produced by the TENG has similar or even better antibacterial effect.

3.2. Effect of TENG stimulation on the initial bacterial adhesion

Gram-positive and gram-negative bacteria are two kinds of pathogens known to form biofilms on the surface of titanium implants, and there are growing concerns over the prevalence of these often antibiotic resistant pathogens being isolated from infected orthopedic implants [55–58]. Therefore, in this study, gram-positive *S. aureus* and gram-negative *E. coli* were selected to evaluate the inhibitory effect of TENG stimulation on both of these kinds of pathogens.

In a pilot study, we compared the antibacterial effects of negatively charged pure Ti and TNT discs at 2 and 6 h, and the result is given in Supplementary Fig. 3. This preliminary result shows that the antibacterial rate of negatively charged TNT was clearly higher than that of the stimulated pure Ti. This may be owing to the pure Ti sheet being conducting, whereas the anodized Ti acted as a parallel-plate capacitor, in which case the negative charge was retained on the surface of the TNT.

Therefore, in the following experiments, we only detected the effects of TENG stimulation on TNT discs.

Fig. 3a shows the result of the crystal violet staining of *E. coli* and *S. aureus* biofilms on the surface of TNT discs with or without TENG stimulation for 2 and 4 h. The quantity of bacteria on the surface of the TNT discs in the TENG groups was slightly lower than that in the control groups in the first 2 h, but without statistically significant differences. This is likely because 2 h is insufficient time for the bacteria to form a biofilm. In addition, short-term contact is not expected to help to kill the bacteria [21]. However, after charging for 4 h, the number of bacteria adhered to the samples in the TENG group was much lower than for the control samples for both *E. coli* and *S. aureus* ($p < 0.05$). The *E. coli* was

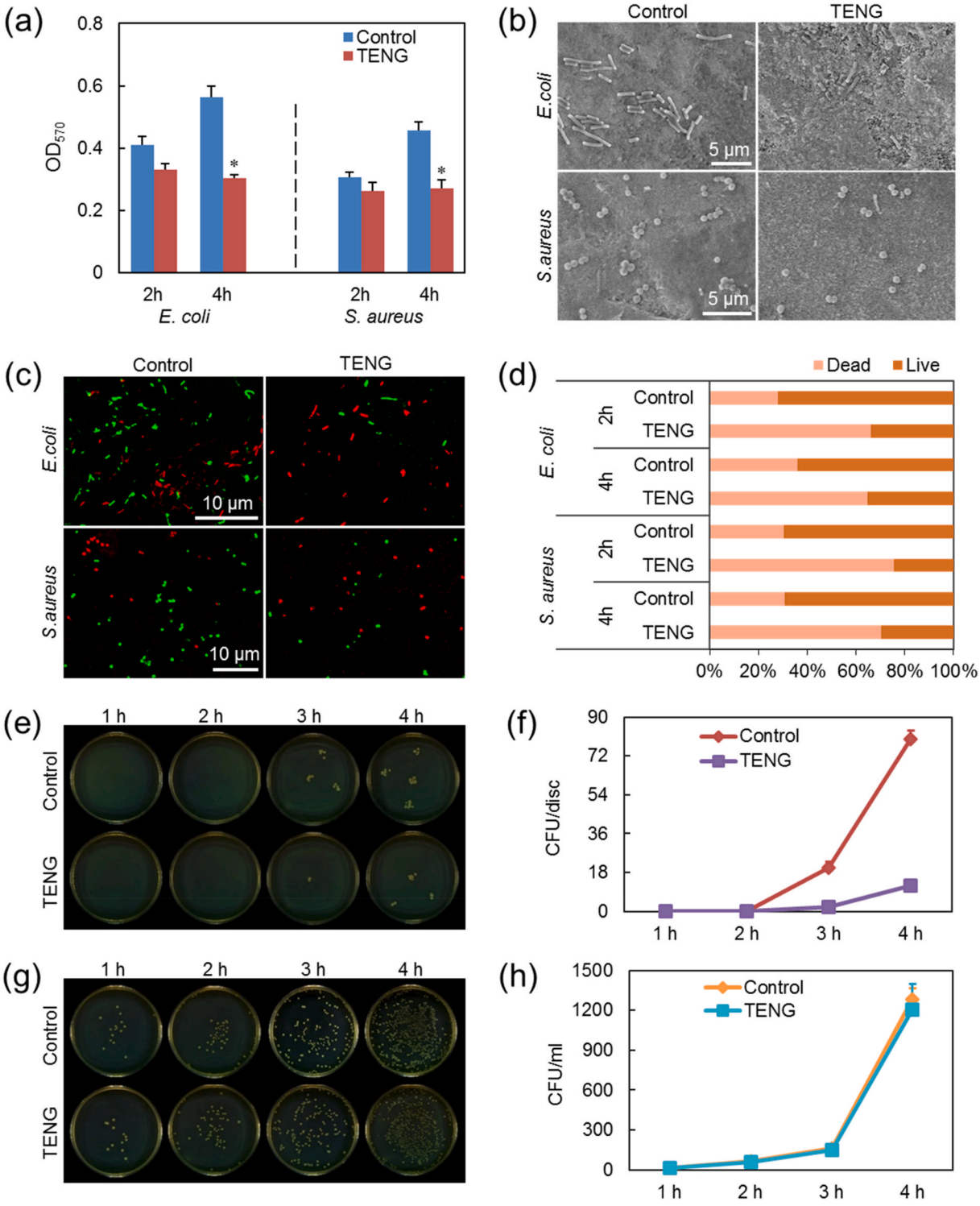

Fig. 3. Effects on biofilm formation on the surface of TNT in the early contact stage (2–4 h). (a) The quantity of bacteria on the surface of TNT after 2 and 4 h was quantified by crystal violet staining (*$p < 0.05$). (b) Bacterial morphology on the TNT was observed by SEM after 4 h. (c) The distribution of bacteria on the TNT after being treated for 4 h was revealed by SYTO 9/PI staining, and (d) the ratio of live/dead bacteria. (e) The bacteria adhered to the surface and (g) bacteria in the culture medium were assessed using the colony counting method and the comparison results are shown separately in (f) and (h). (For interpretation of the references to colour in this figure legend, the reader is referred to the Web version of this article.)

reduced by ~46% and the *S. aureus* was reduced by ~40%. Further results of both SEM (Fig. 3b) and SYTO 9/PI (Fig. 3c) staining further confirmed that the number and density of bacteria for the TENG charged group were lower than those of the control group. Additional statistics were carried out on the proportion of live/dead bacteria and the result is shown in Fig. 3d. Compared with the control group, the proportion of live bacteria decreased significantly in the TENG groups. This observation revealed that in addition to repelling bacteria, the negative charge accumulated on the surface of the TNT disc also had the function of killing bacteria. There is no clear mechanism for the antibacterial activity of electrical stimulation, possible reasons for the observations include formation of electrolysis products (such as H_2O_2, oxidizing radicals, and chlorine molecules), oxidation of enzymes and coenzymes, membrane damage leading to the leakage of cytoplasmic constituents, reduced bacterial respiratory rate, and the introduction of an extra force to stimulate bacterial detachment [59].

To further verify the effect of TENG charging on the inhibition of the initial adhesion of bacteria on the surface of a TNT disc, we quantified the CFU of *E. coli* on the surface of TNT by pasting discs at five different positions in each bacterial Petri dish (Fig. 3e). The number of colonies after 1, 2, 3, and 4 h were counted and the result is summarized in Fig. 3f. Neither the control group nor the TENG charged group had colonies in the Petri dish within the first 2 h. There were only a few individual bacteria on the surface in the first 2 h, and the bacterial biofilm may not yet have formed, which is consistent with the result of crystal violet staining. 3 h later, only one colony appeared on the Petri dish in the TENG charging group, while 18 colonies were present in the control group, which was a statistically significant difference. 4 h later, the number of colonies in the control group was approximately 5 times that of the TENG stimulation group. All of the above results support the finding that the negatively charged surface produced by TENG charging clearly inhibits bacterial adhesion, which helps to delay the formation of bacterial biofilms.

The couple of TNT and Ti discs can be considered as a parallel-plate capacitor, then the capacitance increased as the greater charge storage. Because the potential is applied to the cathodic of flat band potential, excessive negative charges gathered at the electrode interface. According to Hong and Brown's hypothesis [60,61], as a bacteria with functional polar groups exhibits a negative charge surface, electroneutrality requires the opposite charges in the space between the two surfaces. A wave of recent researches have indicated that the electric field generated at polarized electrodes gives rise to hydrated ions to move away from the surface creating an electro-osmotic fluid flow which mechanically disrupts adherent biofilms [59,62,63]. Besides, electrodes can disrupt the charge distribution within the extracellular matrix secreted by bacteria of an adherent biofilm and alter the transport ions and other charged moieties within the biofilm [64].

In addition to the effect of TENG stimulation on biofilm formation on the implant surface, we were also interested in its effects on the bacteria in the tissue fluid around the implant. Therefore, we also measured the change of bacterial number in the culture medium during the first 4 h, and the results are shown in Fig. 3g and h. We found that TENG charging only affects the implant surface but not planktonic bacteria in solution.

Combining the results from Fig. 3a–f, we can conclude that even when TNT discs are exposed to very high concentrations of bacterial solutions, TENG stimulation can delay biofilm formation by preventing the bacteria from adhering to the TNT samples and kill some of the bacteria. Because the concentration of bacteria in tissue and blood is much lower than that used in our experiment, we infer that TENG can effectively inhibit the formation of biofilms by acting on the surface of anodized titanium alloy implants.

3.3. Effect of TENG stimulation on biofilm maturation

From the results in section 3.2, we learned that in both the TENG charged and control groups, the biofilms on the surfaces of samples did not form until 2 h. However, continuous colonies appeared on the surface of the samples in the control group after 4 h, which indicated the initial formation of biofilms. In contrast, only a few sparse colonies adhered to the surface of the samples in the TENG charged group and there was no biofilm formation. Through the work in this section, we attempted to reveal the impact of TENG charging on the process of biofilm formation to maturation, including the changes in biofilm morphology, the number of bacteria, and the proportion of live bacteria in the process. The first 3 days are critical for biofilm formation, and as such we detected the changes in bacterial biofilms from 2 h to 72 h.

Fig. 4a shows the results of semi-quantified analysis of the crystal violet staining of the two model bacteria on the surface of different samples at different time intervals. Statistical analysis showed that the OD value increased approximately three times for *E. coli* and five times for *S. aureus* in the control group, while the OD value increased by less than twice for both bacteria in the TENG charging group. Meanwhile, the number of bacteria on the surface of the TENG charging group was significantly lower than that in the control group at different time intervals, indicating that the growth rate of bacteria on the surface of the TNT disc was significantly inhibited by the negative charging of the TENG. After 72 h of continuous charging, the antibacterial efficiency for *E. coli* reached 72% and that for *S. aureus* reached 65%.

SEM was used to observe the bacterial density and distribution on the surface of the TNT discs. Although the SEM images in Fig. 4 d show that the bacteria adhering to the TNT increased with time, whether they were charged or not, the biofilms formed on the non-charged samples were more continuous and thicker than those on the TENG charged discs as time progressed. For both the gram-positive bacteria *S. aureus* and gram-negative bacteria *E. coli*, the bacterial density of the TENG group at the same observed time point was significantly lower than that of the control group, as the figures show, indicating that TENG stimulation played a more significant inhibitory role on *E. coli* than on *S. aureus*. In addition, both *E. coli* and *S. aureus* showed a sparse colony distribution, even in the TENG charged group after 72 h, however a continuous biofilm formed after only 4 h in the control group. This result shows that the formation time of a continuous bacterial biofilm can be significantly extended after the surface is negatively charged by TENG.

To further understand the changes in bacterial density, live/dead ratio in the biofilm, thickness of the biofilm, and distribution of bacteria as a function of TENG charge, we stained the live and dead bacteria on the surface and observed the samples using laser confocal microscopy. The results are shown in Fig. 4c. The proportion of live/dead bacteria was calculated and the result is shown in Fig. 4b. Statistical analysis showed that after 72 h of TENG stimulation, the live/dead ratios of *E. coli* and *S. aureus* were approximately 20% and 40%, respectively, while they were 55% and 63% in the control group, respectively, illustrating that the proportion of viable bacteria decreased significantly under TENG stimulation. The 3D images of the biofilm on the sample surface are also shown in Fig. 4c, which clearly indicates that there are significant differences in the bacteria amount and live/dead ratio between the TENG charging and the control group. Thus, negative TENG charging not only reduced the total number of bacteria adhered to the surface, but also reduced the proportion of living bacteria, which demonstrated that the negatively charged TNT surface not only repels bacteria, but also kills them. Again, we observed that the negative surface produced by TENG charging was more effective in inhibiting gram-negative bacteria than gram-positive bacteria. This may be the result of the cell wall of gram-positive bacteria (20–80 nm) being thicker than that of gram-negative bacteria (10–15 nm) [65], so they are more difficult to destroy under the action of electric charge [66,67].

Combining the results of crystal violet staining, SEM, and confocal laser scanning images (Fig. 4a–c), we found that in the TENG charging group, the amount of bacteria and the ratio of live/dead bacteria changed little from the biofilm initially formed to the end of our observation, indicating that the biofilm had matured. Meanwhile the number of these two bacteria in the control group increased

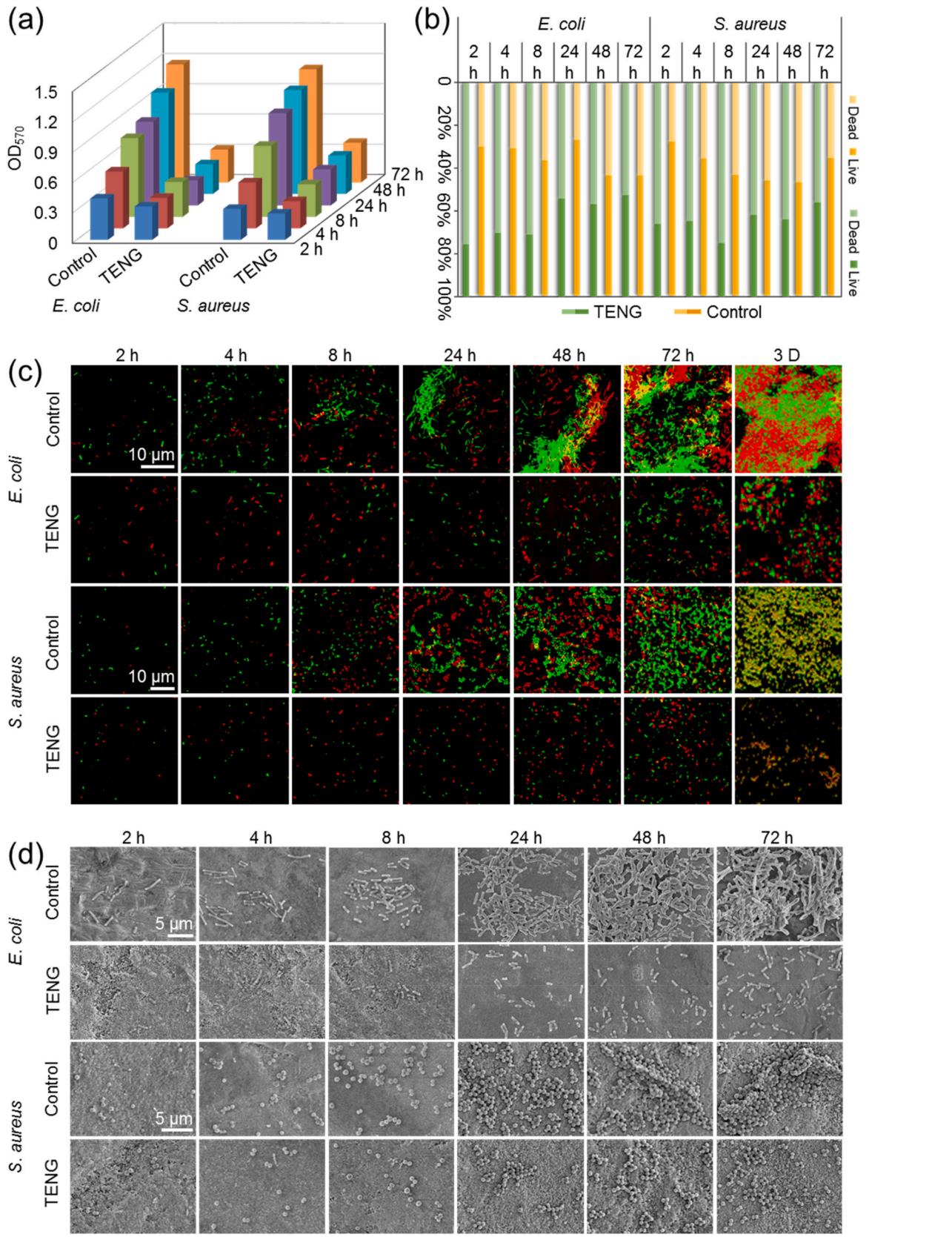

Fig. 4. Anti-biofilm formation effects at different time points (2–72 h). (a) Crystal violet staining analysis of both groups at different points was assessed by microplate reader at 570 nm. (c) LIVE/DEAD staining images of *E. coli* and *S. aureus* on the TNT discs treated with TNT control, and TENG stimulation, and (b) Ratio of live and dead bacteria on the surface of TNT discs. (d) SEM images of *E. coli* and *S. aureus* on the surface of TNT discs. (For interpretation of the references to colour in this figure legend, the reader is referred to the Web version of this article.)

continuously over 72 h, indicating that the bacterial biofilm was still in the process of development. All of the above results demonstrated that the negative charge on the TNT discs introduced by TENG accelerated the maturation of the bacterial biofilm, and effectively reduced the number of bacteria and the proportion of living bacteria in the biofilm.

3.4. Effect of TENG stimulation on the elimination of formed biofilms

We have learned that it is difficult to destroy mature biofilms even with high concentrations of antibiotics because of the protective effect of the biofilm itself on the bacteria. Moreover, the formed bacterial biofilm continuously releases bacteria into the surrounding environment. Therefore, it is necessary to find new techniques to effectively destroy already formed bacterial biofilms, in order to reduce the risk of persistent infection introduced by implants. Therefore, we also studied the effect of TENG electrical stimulation on damaging mature biofilms and the bacteria release profile from the biofilms. The effects of using antibiotics (AB) alone and the combination of TENG and AB were compared with those of using TENG alone.

First, bacteria were cultured with TNT discs without charging for 24 h to form mature biofilms on the surface. The time was selected according to the results in section 3.3. Then, the samples were charged for another 24 h to assess the impact of TENG charging on the already formed biofilm, as well as the planktonic bacteria in the culture medium. This procedure is illustrated in Fig. 5a. Fig. 5b and c showed the effect of TENG, AB and their combined utilization on the number of bacteria released from the formed bacterial biofilm. The images in Fig. 5b directly showed the colonies of bacteria on agar plates in different groups, while Fig. 5c gave the statistical counting results of the colony (CFU/mL) in the culture medium among different groups. Compared with the blank control group, the number of bacteria released into the culture medium in the TENG stimulation group decreased significantly, which may be a result of the amount of live bacteria in the biofilm on the TNT discs in the TENG group being less than that in the control group, leading to a decrease in released bacteria. The results also showed that the antibiotics (AB) kill most of the corresponding sensitive bacteria in the culture medium, but TENG stimulation did not show a significant effect on planktonic bacteria (Fig. 5b and c), which illustrates that negative charge had only a contact repelling interaction or killing effect on bacteria while AB played a key role in killing planktonic bacteria. Furthermore, when TENG and AB were used in combination, the number of bacteria both on the surface and culture medium decreased significantly.

We further semi-quantitatively studied the changes of the bacterial biofilms on the surfaces of TNT discs with different treatments. The OD values of crystal violet staining are given in Fig. 5d. Compared with the control group, the bacteria on the surface of the samples in the TENG charged group decreased by ~70%, however there was no significant difference between the AB and the control group.

In the AB and TENG combined using group, the number of bacteria on the surface markedly decreased when compared with the group only treated with AB, however the result was very close to that observed for samples only treated with TENG. This result further demonstrated that TENG stimulation played a significant role in destroying the bacteria on the surface of the material, while antibiotics showed little effect on the bacteria that were protected by the biofilm. It is well known that antibiotics alone have a weak effect on biofilms, which means that implant-associated infections are difficult to control and treat, and misuse of antibiotics can lead to the emergence of drug-resistant bacterial strains [68]. According to this study, TENG stimulation exhibited a significant effect on promoting the detachment of biofilms.

To further understand the effect of TENG stimulation on the proportion of viable bacteria in a biofilm, we stained the samples with fluorescent dyes. The images are shown in Fig. 5f and the calculated result for the live/dead bacteria ratio is shown in Fig. 5e. Interestingly, regardless of the total amount of bacteria and the proportion of living bacteria, the TENG stimulation group showed a significant decrease when compared with the control group. Compared with the control group, the proportion of living bacteria on the surface of the samples in the TENG charged group decreased from 60% to 20% for *E. Coil* and 30% for *S. aureus*. Antibiotic intervention had no effect on the total number of surface bacteria, but slightly reduced the proportion of living bacteria. When TENG was combined application with AB, the effect of their combination on surface bacteria was similar to that of TENG alone, which further indicated that antibiotics had little effect on biofilms, but TENG significantly reduced the number of bacteria and the proportion of live bacteria on the surface.

Summarizing the above results, the AB were effective for killing the planktonic bacteria, however it was difficult to detach biofilms from the plate surfaces with AB. In contrast, TENG stimulation was able to kill most of the bacteria in the biofilm. This study reveals a new way of treating biofilm related infection. It can be predicted that this TENG produced electrical charging method would be supplied as an assistant treatment with widespread antibiotic therapy. It can not only destroy bacterial biofilms formed on the implant surface effectively, but also kill the planktonic bacteria released into the surrounding tissues and prevent the formation of new bacterial biofilms through the combination method. Currently the most effective clinical treatments for dealing with implant-related infections invariably use of antibiotics, this study gives a new choice to combine the TENG charging method with antibiotics, which will make this technology a more clinically relevant therapeutic approach.

3.5. Effect of TENG stimulation on MC3T3-E1

Bioelectricity is an important biological signal in the function of all living organisms. Therefore, external electrical stimuli is also proved to be an attractive guiding signal for affecting cell behavior and further promoting tissue regeneration [69]. The capacitively coupled electric field [70] and the biphasic current stimulation system [71] have been shown to be effective methods of promoting bone fracture healing, and enhancing the proliferation and differentiation of precursor cells or stem cells. The purpose of this study is to verify the effect of the continuous negative charge generated on the surface of oxidized titanium-based implants on the behavior of preosteoblasticMC3T3-E1 by transforming the force generated by normal human activities into electricity through TENG.

The morphology of MC3T3-E1, which adhered to surfaces in all groups, was observed by SEM, as shown in Fig. 6a. MC3T3-E1 cells spread well on all of the samples. Notably, the cells on the pure Ti and TNT discs without electrical stimulation retained their original shape after culturing for 5 days, whereas those on the TNT discs stimulated by TENG exhibited more and longer filopodia than other groups. Fluorescent staining was utilized to show the cytoskeleton of MC3T3-E1 cells (Fig. 6b). The cells on the surface of TNT with or without TENG stimulation exhibited a greater spread with a larger distribution of the actin cytoskeleton than those on the Ti discs. Moreover, more connected actin fibers, which are beneficial to intercellular communication, could be seen around the cells in both the TENG+ and TENG− groups.

The viability and proliferation of pre-osteoblast MC3T3-E1 were evaluated by CCK-8 assay and the result is shown in Fig. 6c. The proliferation and differentiation of cells on pure Ti, TNT, TENG− (negatively charged TNT surface), and TENG+ (positively charged TNT surface) discs were good. The formation of nanotube arrays by surface anodization can significantly promote cell proliferation. It is believed that the increase of surface roughness and specific surface area are the main reasons according to other reports [72,73]. However, there were no significant differences between the OD values for the TENG charged and other groups, whether the surface of TNT was positively or negatively charged ($p > 0.05$). This result effectively demonstrates that electrical stimulation generated by TENG was harmless to MC3T3-E1.

ALP activity is an impotent marker that reflects the differentiation

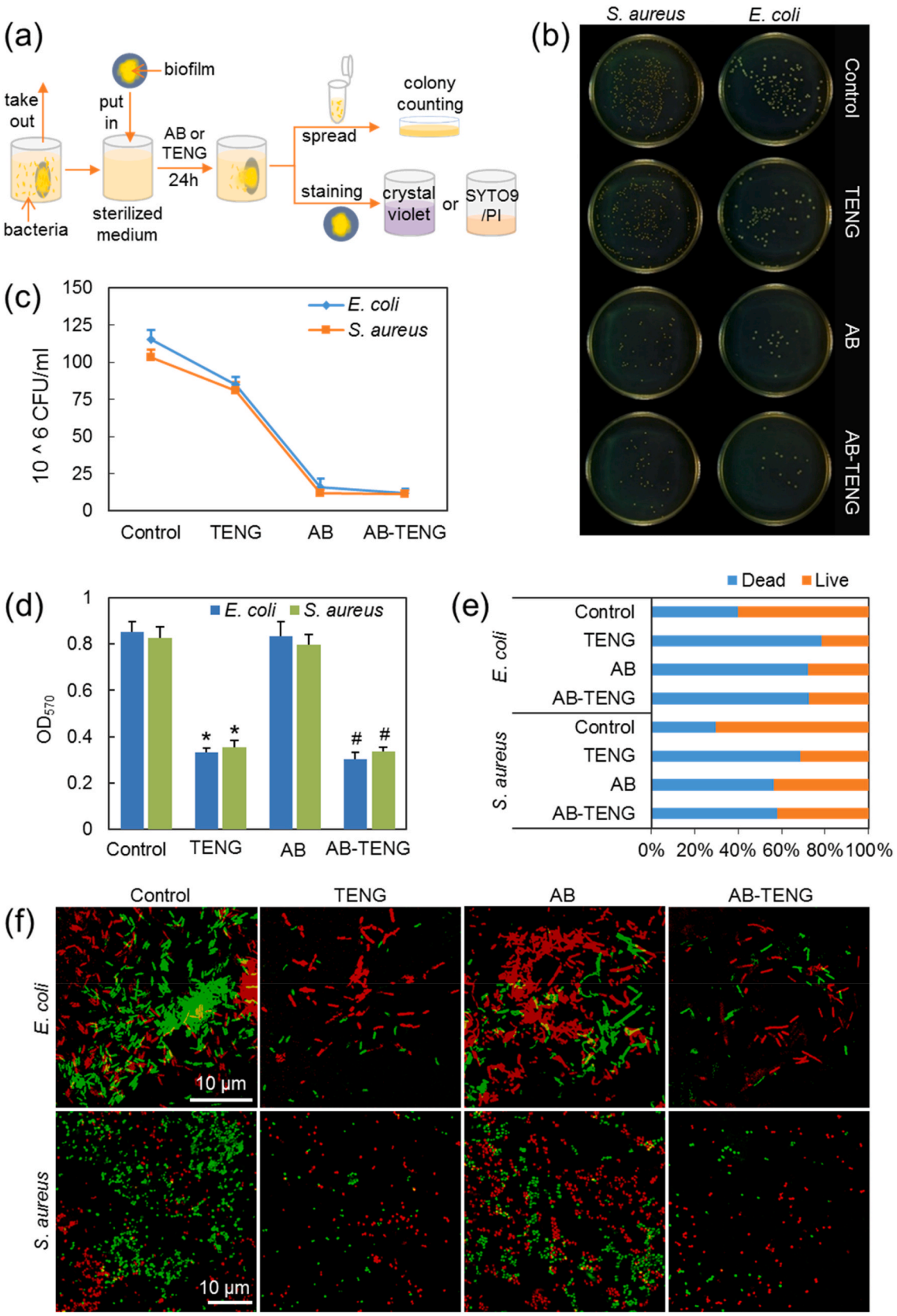

Fig. 5. Effects of TENG, AB and their combined utilization on the bacteria release from the pre-formed biofilms and elimination of formed bacterial biofilm on the surface of TNTs. (a) Experimental processes before colony counting. (b) Images of colony counting by use of different culture medium. (c) Statistical counting results of the colony (CFU/mL) in the culture medium. (d) OD values of crystal violet staining analysis of *E. coli* and *S. aureus* biofilms treated with TNT control, TENG charging, AB, and their combined utilization after 24 h $^{*}p < 0.05$ compared with control group, $^{\#}p < 0.05$ compared with AB group. (f) LIVE/DEAD staining images of bacteria on the surface of TNT discs and (e) the ratio of live and dead bacteria by analysis of average fluorescence intensity in Fig. 5(f). (For interpretation of the references to colour in this figure legend, the reader is referred to the Web version of this article.)

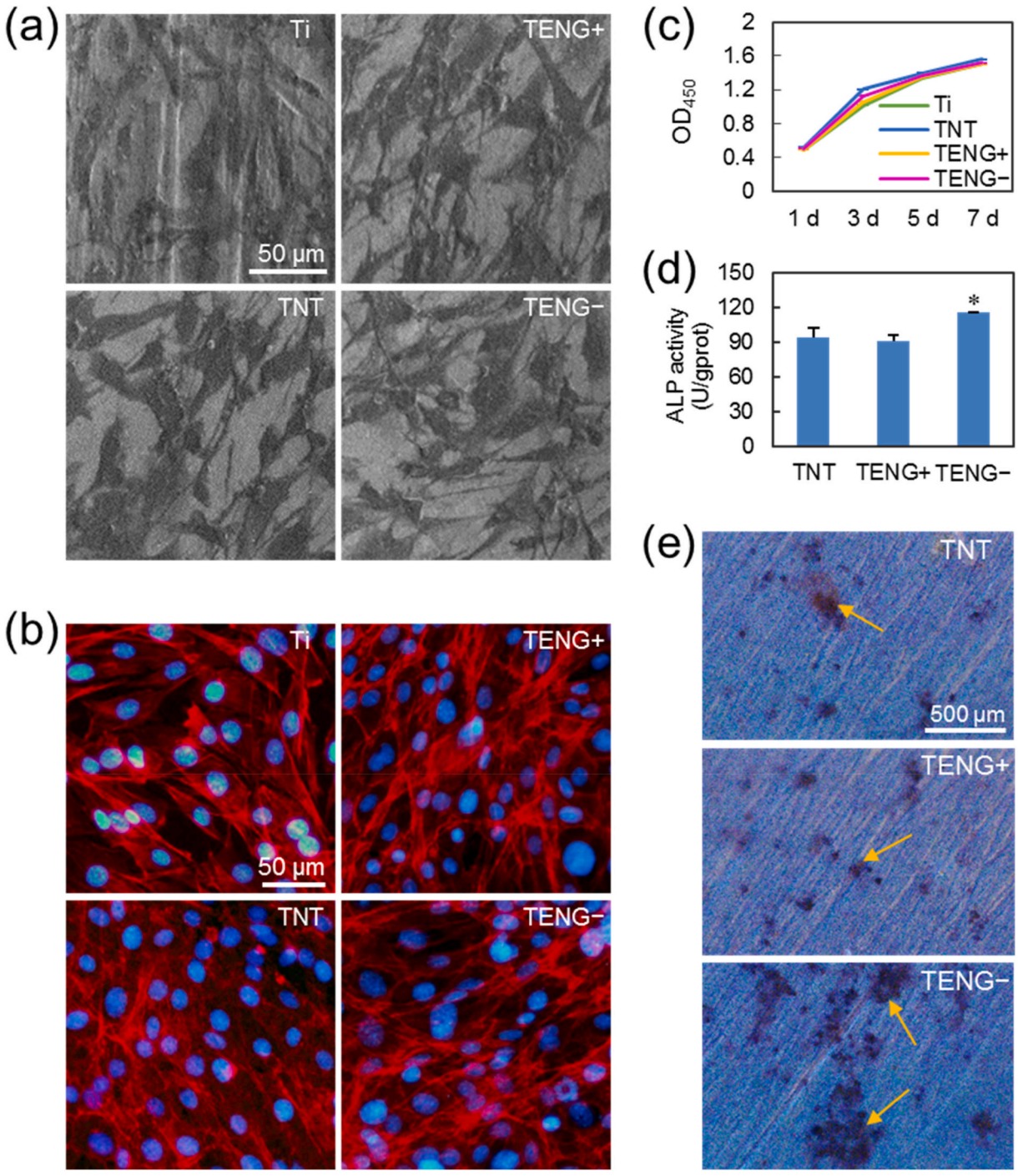

Fig. 6. Effects of TENG on MC3T3-E1 proliferation and osteogenic differentiation. (a) SEM images of MC3T3-E1 on different surfaces, (b) Phalloidin (red) and Hoechst 33,258 (blue) staining of F-actin and nuclei of MC3T3-E1 cells, respectively, after treating for 5 days. (c) CCK-8 analysis of MC3T3-E1 treated with Ti, TNT, TENG− (negatively charged Ti/TNT surface), and TENG+ (positively charged Ti/TNT surface). (d) ALP activity test of the cells treated with TNT, TENG−, and TENG + after 7 days. (e) Calcium deposits with alizarin red staining of MC3T3-E1 after treatment for 21 days. (For interpretation of the references to colour in this figure legend, the reader is referred to the Web version of this article.)

level of osteoblasts. After being cultured for 7 days on the TNT discs with or without TENG charging, MC3T3-E1 cells were harvested and the ALP activity of these cells was detected. As shown in Fig. 6d, there is no difference between the non-charged samples (TNT group) and the samples with positively charged surfaces (the TENG + group); however the ALP activity of cells on the negatively charged surface (the TENG− group) was significantly enhanced compared with the other groups, which indicates that the degree of differentiation of MC3T3-E1 was higher than that in the other two groups. Calcium deposition is another important marker of osteogenic differentiation that manifests later than ALP secretion, thus the calcium mineralization of the cells was also evaluated by alizarin red staining. As illustrated in Fig. 6e, there were no significant differences in the number of calcium nodules between the TNT and TENG + groups, whereas the number of nodules in the TENG− group was much greater than those in the other two groups. Based on the above study, MC3T3-E1 cells on the negatively charged surface of TNT discs were more likely to differentiate into osteoblasts. Previous studies indicated that osteoblasts were more active near the cathode [31,74].

The mechanism may be related to the slightly alkaline environment caused by the increasing pH level around the cathode, which has been postulated as favorable for bone growth [30].

4. Conclusion

In this study, mechanical energy generated by human physiological movement was collected by a TENG and converted into electrical energy, which was then transferred to the anodized titanium to construct a negatively charged implant surface. The advantages of this self-powered method are obvious. Without introducing any new materials, this method shows stable and effective activities of antibacterial and *anti*-biofilms. This negative-charged surface significantly prevented the adhesion of gram-positive and gram-negative organisms, and inhibited the formation of biofilms. In addition, the number of bacteria and the proportion of live bacteria in already formed biofilms were greatly reduced. Mature bacterial biofilms were also effectively destroyed as a function of self-powered electrical stimulation. Meanwhile, the electrical signals generated by the TENG markedly promoted preosteoblast adhesion, osteogenic differentiation and proliferation. The treated implant reveals osteogenesis promotion in MC3T3-E1 cells, without adverse effects. This study provides a basis for future research into the application of TENG in orthopedics and may be important for orthopedic or dental implants owing to the sustainable *anti*-biofilm activity and osteogenesis promotion demonstrated.

Declaration of competing interest

The authors declare that they have no known competing financial interests or personal relationships that could have appeared to influence the work reported in this paper.

CRediT authorship contribution statement

Rui Shi: Investigation, Writing - review & editing. **Jingshuang Zhang:** Data curation, Investigation. **Jingjing Tian:** Investigation. **Chaochao Zhao:** Investigation. **Zhe Li:** Investigation. **Yingzi Zhang:** Writing - review & editing. **Yusheng Li:** Writing - review & editing. **Chengai Wu:** Methodology. **Wei Tian:** Project administration. **Zhou Li:** Writing - review & editing.

Acknowledgment

The authors thank the support of the National Natural Science Foundation of China (No. 51673029, 61875015, 21801019), National Key R&D Project from Minister of Science and Technology, China (2016YFA0202703), the Beijing Municipal Health Commission (PXM2020-026275-000003; BMHC2018-4; BMHC2019-9), Beijing Talent Fund (grant number 2016000021223ZK34), Beijing Nova Programme Interdisciplinary Cooperation Project (Z191100001119012); the Beijing Natural Science Foundation (7204333), the University of Chinese Academy of Sciences and the National Youth Talent Support Program.

Appendix A. Supplementary data

Supplementary data to this article can be found online at https://doi.org/10.1016/j.nanoen.2020.105201.

References

[1] F. Parnia, J. Yazdani, V. Javaherzadeh, S. Maleki Dizaj, J. Pharm. Pharmaceut. Sci. 20 (2017) 148–160.
[2] N. Jiang, Z. Guo, D. Sun, Y. Li, Y. Yang, C. Chen, L. Zhang, S. Zhu, ACS Nano 12 (2018) 7883–7891.
[3] H. Chouirfa, H. Bouloussa, V. Migonney, C. Falentin-Daudre, Acta Biomater. 83 (2019) 37–54.
[4] R. Wang, K.G. Neoh, Z. Shi, E.T. Kang, P.A. Tambyah, E. Chiong, Biotechnol. Bioeng. 109 (2012) 336–345.
[5] J.W. Costerton, B. Ellis, K. Lam, F. Johnson, A.E. Khoury, Antimicrob. Agents Chemother. 38 (1994) 2803–2809.
[6] L.G. Harris, S. Tosatti, M. Wieland, M. Textor, R.G. Richards, Biomaterials 25 (2004) 4135–4148.
[7] T.P. Schaer, S. Stewart, B.B. Hsu, A.M. Klibanov, Biomaterials 33 (2012) 1245–1254.
[8] S.J. Lee, D.N. Heo, H.R. Lee, D. Lee, S.J. Yu, S.A. Park, W.K. Ko, S.W. Park, S.G. Im, J.H. Moon, I.K. Kwon, J. Mater. Chem. B 3 (2015) 5161–5165.
[9] K.V. Holmberg, M. Abdolhosseini, Y. Li, X. Chen, S.U. Gorr, C. Aparicio, Acta Biomater. 9 (2013) 8224–8231.
[10] D. Campoccia, L. Montanaro, C.R. Arciola, Biomaterials 34 (2013) 8533–8554.
[11] S. He, P. Zhou, L. Wang, X. Xiong, Y. Zhang, Y. Deng, S. Wei, J. R. Soc. Interface 11 (2014), 20140169.
[12] S.W. Park, D. Lee, S.C. Yong, H.B. Jeon, C.H. Lee, J.H. Moon, I.K. Kwon, Appl. Surf. Sci. 303 (2014) 140–146.
[13] J. Gallo, M. Holinka, C.S. Moucha, Int. J. Mol. Sci. 15 (2014) 13849–13880.
[14] B. Gottenbos, D.W. Grijpma, H.C. van der Mei, J. Feijen, H.J. Busscher, J. Antimicrob. Chemother. 48 (2001) 7–13.
[15] B. Zdyrko, V. Klep, X. Li, K. Qian, S. Minko, X. Wen, I. Luzinov, Mater. Sci. Eng. C 29 (2009) 680–684.
[16] O. Rzhepishevska, S. Hakobyan, R. Ruhal, J. Gautrot, D. Barbero, M. Ramstedt, Biomater Sci 1 (2013) 589–602.
[17] G. Wang, H. Feng, L. Hu, W. Jin, Q. Hao, A. Gao, X. Peng, W. Li, K.Y. Wong, H. Wang, Z. Li, P.K. Chu, Nat. Commun. 9 (2018) 2055.
[18] J. Tian, H. Feng, L. Yan, M. Yu, H. Ouyang, H. Li, W. Jiang, Y. Jin, G. Zhu, Z. Li, Nano. Energy 36 (2017) 241–249.
[19] H. Murata, R.R. Koepsel, K. Matyjaszewski, A.J. Russell, Biomaterials 28 (2007) 4870–4879.
[20] H. Strahl, L.W. Hamoen, Proc. Natl. Acad. Sci. U. S. A. 107 (2010) 12281–12286.
[21] A. Terada, K. Okuyama, M. Nishikawa, S. Tsuneda, M. Hosomi, Biotechnol. Bioeng. 109 (2012) 1745–1754.
[22] X. Zhao, T. Wang, S. Qian, X. Liu, J. Sun, B. Li, Int. J. Mol. Sci. 17 (2016) 292.
[23] H.K. Tsou, M.H. Chi, Y.W. Hung, C.J. Chung, J.L. He, BioMed Res. Int. 2015 (2015), 328943.
[24] S. Facca, D. Lahiri, F. Fioretti, N. Messadeq, D. Mainard, N. Benkirane-Jessel, A. Agarwal, ACS Nano 5 (2011) 4790–4799.
[25] R.S. Bedi, L.P. Zanello, Y. Yan, Adv. Funct. Mater. 19 (2009) 3856–3861.
[26] R. Olivares-Navarrete, S.L. Hyzy, D.L. Hutton, C.P. Erdman, M. Wieland, B. D. Boyan, Z. Schwartz, Biomaterials 31 (2010) 2728–2735.
[27] C. Zhao, P. Cao, W. Ji, P. Han, J. Zhang, F. Zhang, Y. Jiang, X. Zhang, J. Biomed. Mater. Res. 99 (2011) 666–675.
[28] R. Olivares-Navarrete, R.A. Gittens, J.M. Schneider, S.L. Hyzy, D.A. Haithcock, P. F. Ullrich, Z. Schwartz, B.D. Boyan, Spine J. 12 (2012) 265–272.
[29] W. Liu, N.H. Golshan, X. Deng, D.J. Hickey, K. Zeimer, H. Li, T.J. Webster, Nanoscale 8 (2016) 15783–15794.
[30] B.M. Isaacson, L.B. Brunker, A.A. Brown, J.P. Beck, G.L. Burns, R.D. Bloebaum, J. Biomed. Mater. Res. B Appl. Biomater. 97 (2011) 190–200.
[31] B.Y. Yang, T.C. Huang, Y.S. Chen, C.H. Yao, Evidence-based Complementary and Alternative Medicine, vol. 2013, eCAM, 2013, p. 607201.
[32] K.E. Hammerick, A.W. James, Z. Huang, F.B. Prinz, M.T. Longaker, Tissue Eng. 16 (2010) 917–931.
[33] D. Kaynak, R. Meffert, M. Gunhan, O. Gunhan, J. Periodontol. 76 (2005) 2194–2204.
[34] T. Zhang, M. Zhang, Y. Fu, Y. Han, H. Guan, H. He, T. Zhao, L. Xing, X. Xue, Y. Zhang, Y. Zhan, Nano. Energy 63 (2019), 103884.
[35] H. He, Y. Fu, W. Zang, Q. Wang, L. Xing, Y. Zhang, X. Xue, Nano. Energy 31 (2017) 37–48.
[36] H. Guan, D. Lv, T. Zhong, Y. Dai, L. Xing, X. Xue, Y. Zhang, Y. Zhan, Nano. Energy 67 (2020) 104182.
[37] Y. Zhang, Z. Zhou, L. Sun, Z. Liu, X. Xia, T.H. Tao, Adv. Mater. 30 (2018), e1805722.
[38] T. Chen, Q. Shi, M. Zhu, T. He, L. Sun, L. Yang, C. Lee, ACS Nano 12 (2018) 11561–11571.
[39] Z. Li, H. Feng, Q. Zheng, H. Li, C. Zhao, H. Ouyang, S. Noreen, M. Yu, F. Su, R. Liu, Nano. Energy 54 (2018) 390–399.
[40] Q. Zheng, B. Shi, Z. Li, Z.L. Wang, Adv. Sci. 4 (2017), 1700029.
[41] H. Feng, C. Zhao, P. Tan, R. Liu, X. Chen, Z. Li, Adv Healthc Mater 7 (2018), e1701298.
[42] X. Pu, H. Guo, J. Chen, X. Wang, Y. Xi, C. Hu, Z.L. Wang, Science Advances 3 (2017), e1700694.
[43] G.T. Hwang, H. Park, J.H. Lee, S. Oh, K.I. Park, M. Byun, H. Park, G. Ahn, C. K. Jeong, K. No, H. Kwon, S.G. Lee, B. Joung, K.J. Lee, Adv. Mater. 26 (2014) 4880–4887.
[44] Y. Ma, Q. Zheng, Y. Liu, B. Shi, X. Xue, W. Ji, Z. Liu, Y. Jin, Y. Zou, Z. An, W. Zhang, X. Wang, W. Jiang, Z. Xu, Z.L. Wang, Z. Li, H. Zhang, Nano Lett. 16 (2016) 6042–6051.
[45] Q. Zheng, B. Shi, F. Fan, X. Wang, L. Yan, W. Yuan, S. Wang, H. Liu, Z. Li, Z. L. Wang, Adv. Mater. 26 (2014) 5851–5856.
[46] D.Y. Park, D.J. Joe, D.H. Kim, H. Park, J.H. Han, C.K. Jeong, H. Park, J.G. Park, B. Joung, K.J. Lee, Adv. Mater. (2017) 29.
[47] H. Ouyang, J. Tian, G. Sun, Y. Zou, Z. Liu, H. Li, L. Zhao, B. Shi, Y. Fan, Y. Fan, Z. L. Wang, Z. Li, Adv. Mater. 29 (2017).

[48] Q. Zheng, H. Zhang, B. Shi, X. Xue, Z. Liu, Y. Jin, Y. Ma, Y. Zou, X. Wang, Z. An, W. Tang, W. Zhang, F. Yang, Y. Liu, X. Lang, Z. Xu, Z. Li, Z.L. Wang, ACS Nano 10 (2016) 6510–6518.
[49] C. Park, G. Song, S.M. Cho, J. Chung, Y. Lee, E.H. Kim, M. Kim, S. Lee, J. Huh, C. Park, Adv. Funct. Mater. 27 (2017).
[50] Albert T. Poortinga, Rolf Bos, Willem Norde, Henk J. Busscher, Surf. Sci. Rep. 47 (5) (2002) 1–32.
[51] M. Canty, N. Luke-Marshall, A. Campagnari, M. Ehrensberger, Acta Biomater. 48 (2017) 451–460.
[52] X. Zhang, C. Zhang, Y. Lin, P. Hu, Y. Shen, K. Wang, S. Meng, Y. Chai, X. Dai, X. Liu, Y. Liu, X. Mo, C. Cao, S. Li, X. Deng, L. Chen, ACS Nano 10 (2016) 7279–7286.
[53] X. Pu, H. Guo, Q. Tang, J. Chen, L. Feng, G. Liu, X. Wang, Y. Xi, C. Hu, Z.L. Wang, Nano. Energy 54 (2018) 453–479.
[54] B. Ercan, K.M. Kummer, K.M. Tarquinio, T.J. Webster, Acta Biomater. 7 (2011) 3003–3012.
[55] J. Parvizi, I.M. Pawasarat, K.A. Azzam, A. Joshi, E.N. Hansen, K.J. Bozic, J. Arthroplasty 25 (2010) 103–107.
[56] K.A. Brossard, A.A. Campagnari, Infect. Immun. 80 (2012) 228–233.
[57] R.A. Bonomo, D. Szabo, Clin. Infect. Dis. 43 (2006) S49–S56.
[58] D.T. Tsukayama, R. Estrada, R.B. Gustilo, J Bone Joint Surg Am 78 (1996) 512–523.
[59] J.L. del Pozo, M.S. Rouse, J.N. Mandrekar, J.M. Steckelberg, R. Patel, Antimicrob. Agents Chemother. 53 (2009) 41–45.
[60] Y. Hong, D.G. Brown, Langmuir 24 (2008) 5003–5009.
[61] Y. Hong, D.G. Brown, Biotechnol. Bioeng. 105 (2010) 965–972.
[62] A.T. Poortinga, J. Smit, H.C. van der Mei, H.J. Busscher, Biotechnol. Bioeng. 76 (2001) 395–399.
[63] A.J. van der Borden, H. van der Werf, H.C. van der Mei, H.J. Busscher, Appl. Environ. Microbiol. 70 (2004) 6871–6874.
[64] S.A. Blenkinsopp, A.E. Khoury, J.W. Costerton, Appl. Environ. Microbiol. 58 (1992) 3770–3773.
[65] G.K. Auer, D.B. Weibel, Biochemistry 56 (2017) 3710–3724.
[66] G. Daeschlein, O. Assadian, L.C. Kloth, C. Meinl, F. Ney, A. Kramer, Wound Repair Regen. 15 (2007) 399–403.
[67] M.K. Canty, L.A. Hansen, M. Tobias, S. Spencer, T. Henry, N.R. Luke-Marshall, A. A. Campagnari, M.T. Ehrensberger, mSphere (2019) 4.
[68] H.M. Han, R. Gopal, Y. Park, Amino Acids 48 (2016) 505–522.
[69] R. Balint, N.J. Cassidy, S.H. Cartmell, Tissue Eng. B Rev. 19 (2013) 48–57.
[70] H. Zhuang, W. Wang, R.M. Seldes, A.D. Tahernia, H. Fan, C.T. Brighton, Biochem. Biophys. Res. Commun. 237 (1997) 225–229.
[71] I.S. Kim, J.K. Song, Y.M. Song, T.H. Cho, T.H. Lee, S.S. Lim, S.J. Kim, S.J. Hwang, Tissue Eng. 15 (2009) 2411–2422.
[72] Z. Lewandowska, P. Piszczek, A. Radtke, T. Jedrzejewski, W. Kozak, B. Sadowska, J. Mater. Sci. Mater. Med. 26 (2015) 163.
[73] E. Beltran-Partida, A. Moreno-Ulloa, B. Valdez-Salas, C. Velasquillo, M. Carrillo, A. Escamilla, E. Valdez, F. Villarreal, Materials 8 (2015) 867–883.
[74] R.A. Gittens, R. Olivares-Navarrete, R. Rettew, R.J. Butera, F.M. Alamgir, B. D. Boyan, Z. Schwartz, Bioelectromagnetics 34 (2013) 599–612.